buildings

Article

Characterization and Analysis of Iron Ore Tailings Sediments and Their Possible Applications in Earthen Construction

Sofia Bessa [1], Marlo Duarte [2], Gabriela Lage [1], Isabela Mendonça [1], Roberto Galery [2], Rochel Lago [3], Ana Paula Texeira [3], Fernando Lameiras [4] and Maria Teresa Aguilar [2,*]

1 School of Architecture, Federal University of Minas Gerais, Belo Horizonte 30130-141, Brazil; sofiabessa@ufmg.br (S.B.); gabrielat@ufmg.br (G.L.); isabelakaroline4@gmail.com (I.M.)
2 School of Engineering, Federal University of Minas Gerais, Belo Horizonte 31270-901, Brazil; marloduarte.eng@gmail.com (M.D.); rgalery@demin.ufmg.br (R.G.)
3 Chemistry Department, Institute of Exact Sciences, Federal University of Minas Gerais, Belo Horizonte 31270-901, Brazil; rochel@ufmg.br (R.L.); anapct@ufmg.br (A.P.T.)
4 Nuclear Technology Development Center, Belo Horizonte 31270-901, Brazil; fsl@cdtn.br
* Correspondence: teresa@ufmg.br

Abstract: Mineral extraction is of ultimate importance for the economies of different countries, and Brazil is one of the world's leading producers of iron ores. Unfortunately, dams are still the main problem, mainly in Minas Gerais, especially after the Fundão Dam rupture in 2015. Additionally, there is still a massive presence of buildings built on earth throughout the Minas Gerais mining region, built from the 18th century to today. Investigating the potential of iron ore tailings (IOT) to be incorporated into traditional earthen construction techniques in regions affected by dam ruptures presents a relevant and innovative research approach. In addition, the local reuse of these sediments should be the priority. Thus, the main objective of this work was to collect, characterize, and analyze the possibilities of the application of these tailings to produce rammed earth (RE). A complete characterization analysis was performed on the samples collected at three points. To analyze the soil-IOT compatibility, representative mixtures of RE were produced, and the specific mass, compaction, and compressive strength were performed. It was observed that the IOT samples have a high silica content and that the mixtures of IOT–soil, even without cement, reached the compressive strength values of the international standards, or even above them.

Keywords: mining wastes; rammed earth; toxicity; mechanical analysis

Citation: Bessa, S.; Duarte, M.; Lage, G.; Mendonça, I.; Galery, R.; Lago, R.; Texeira, A.P.; Lameiras, F.; Aguilar, M.T. Characterization and Analysis of Iron Ore Tailings Sediments and Their Possible Applications in Earthen Construction. *Buildings* **2024**, *14*, 362. https://doi.org/10.3390/buildings14020362

Academic Editor: Grzegorz Ludwik Golewski

Received: 8 December 2023
Revised: 11 January 2024
Accepted: 18 January 2024
Published: 29 January 2024

1. Introduction

Mineral extraction activity is an important operation for the economy of different countries. In this context, Brazil, Australia, and China are among the world's main iron ore producers [1]. According to data from IBRAM [2], Brazil's mining sector revenue reached BRL 209 billion (Brazilian real—BRL) in 2020. Iron ore was responsible for 66% of total revenue, with BRL 138 billion.

A significant portion of the occupation of Minas Gerais emerged in the 17th century due to gold exploration, which continued until the second half of the 18th century. The extraction of iron ore, starting in the 20th century, was the main factor that led industries such as Vale, Samarco, and Alcan to establish themselves in the region and intensely urbanize and occupy various municipalities.

For every ton of iron ore processing in Brazil, around 400 kg of tailings is generated [3]. One possible use of these tailings is the construction of mining dams, where these materials are disposed of as pulp or mud [4]. In Brazil, there are about 870 mining dams; of these, only 50% are included in the national dam safety policy [5].

Minas Gerais is a state in Brazil where the iron ore extraction industry is a considerable necessity for the economy. Starting in the 20th century, iron extraction in the state was the main factor that led industries such as Vale, Samarco, and Alcan to establish themselves in the region and intensely urbanize and occupy various municipalities. As a result of the operation of these companies in Minas Gerais, there are several tailing dams. Some dams have been uncharacterized in Minas Gerais since the last accident occurred in Brumadinho/MG in 2019. Currently, 12 dams have already been uncharacterized [6].

1.1. Iron Ore Tailings

Unfortunately, dams are still the main problem that mining companies face, especially after the rupture of the Fundão Dam, which happened in 2015 in Bento Rodrigues (a subdistrict of the municipality of Mariana, MG). This rupture caused the displacement of tailings and mud through the Gualaxo do Norte, Carmo, and Doce Rivers for 663 km. Thirty-nine municipalities were affected, most of which were in Minas Gerais as well as three in Espírito Santo state [7]. The mud splashed for nearly 17 days [8] until it reached the Atlantic Ocean. Tailings strongly change the rivers' sediment composition and can lead to long-term contamination of biological specimens. Even after seven years, it is important to quantify changes in the ecosystem by observing the environment and characterization of sediment and soil samples in places that had had contact with the mud.

A large part of the tailings displaced by the Rio Doce was retained in the Risoleta Neves hydroelectric plant, also known as Candonga, located 113 km away from the Fundão dam, thus paralyzing its operation. The process of dredging, compaction, and transport to the stacking areas has been carried out by the Renova Foundation since 2016 in the Gualaxo do Norte River and Risoleta Neves hydroelectric plant [9]. However, only in February 2023 were hydroelectric plant activities resumed in the testing phase, and they were reopened for commercial functions after this phase had been concluded. Another part of the tailings accumulated where the mud passed has transformed the relief, landscape, and local soil composition.

In this scenario, the search for new ways of tailing disposal from the iron mining process has been the focus of different research. Some studies point to the feasibility of inserting these samples in construction materials [10], such as applying iron ore tailings (IOT) as a substitute for natural fine aggregate [11]. Iron ore tailings have also been applied as a partial substitute for cement in concrete [12,13], in colored mortars [14] in the production of pigments for paints [15], in the manufacture of bricks [16,17], in the production of microconcretes [18], and as a precursor in the synthesis of geopolymers [19–22].

A deeper concern about their physicochemical properties is necessary before understanding how to use them and develop technologies using these wastes. The accumulated tailings in rivers, dredged and stocked, have been changed and can no longer be treated as dam tailings. It is important to understand that this material is a tailing sediment, so it is not possible to compare it with iron ore tailings taken from the dam [23].

Since the rupture that occurred in Mariana, characterization studies of the sedimented tailings have been carried out [16,24–29]. New characterization studies must be carried out because of the time that the material is in the environment, deposited in the soil and at the bottom of rivers as sediments. In addition, the local reuse of these sediments should be the priority, as it eliminates the environmental and economic impact of transporting this material and strengthens income generation with new products that can be consumed locally.

1.2. The Use of Wastes in Earthen Components

Earth has been a building material for thousands of years due to its abundance and widespread availability. It is found worldwide and can be utilized in different forms and consistencies. In addition to traditional use, earth is a promising material that can offer sustainable solutions due to significant reductions in environmental impact, as well as economic benefits for building construction, as material extraction and transportation costs are minimized due to wide availability at construction sites. Furthermore, building with earth presents environmental benefits by requiring less energy, producing less waste, and reducing fossil fuel burning during production, reducing greenhouse gas emissions such as carbon [30].

However, using earth as a building material may present challenges, especially regarding strength and durability. This is being overcome by incorporating other materials, which may be used as stabilizers to improve the properties of earth components and not affect the environmental impact, such as cement. Concerning contemporary earthen construction techniques, rammed earth (RE) stands out internationally [31]. This mixing process for RE aims to obtain greater dough consistency. It is also known that the soil chosen must have a mixture of sand and clay to obtain greater agglutination and less chance of disintegration of the material [30,31]. Soil stabilization, in the case of architecture, means improving structural parameters, such as compressive strength and durability of the building [32].

When rammed earth is not stabilized, the walls may suffer damage caused by erosion and water ingress, which can cause cracks if not adequately protected. On the other hand, incorporating additives into the earth mixture makes the material more resistant. Some of them are lime, cement, or biopolymers, reducing the need for maintenance and repairs [31]. Several residual materials have been researched as soil stabilizers to produce RE [31,33,34] and adobe [35,36], but not yet IOT. Cementitious stabilization in RE has been widely employed in recent years to improve its durability. The addition of cement or lime as stabilizers increases the rammed earth's strength and reduces shrinkage and wall disintegration [31]. This might be more effective in reinforced RE walls [37], preventing corrosion of the structural reinforcement. According to Kariyawasam and Jayasinghe [38], contents above 4% of cement are desirable for RE construction in tropical climates, and they also suggest that the use of up to 10% cement as a stabilizer still results in lower embodied energy compared to ceramic brick construction.

Rammed earth construction stabilized with cement achieves values of one-third of the embodied energy of conventional masonry construction [39]. Thus, RE construction with low cement addition is considered sustainable [38]. According to Arrigoni et al. [31], incorporating cement as a stabilizer increases the durability of RE, but the same author recommends the use of alternative materials to cement as stabilizers to achieve even lower embodied energy values [31].

Regarding waste materials, some studies indicate that the environmental impacts can be similar between unstabilized RE and RE stabilized with waste materials when the local soil is not suitable on its own [31]. Kosarimovahhed and Toufigh [40] and Giuffrida, Camponetto, and Cuomo [41] pointed out the importance of using waste materials to stabilize soil for RE construction so that the technique continues to be considered low impact. Moreover, the use of waste materials to improve the properties of RE has already been presented by several authors, including fly ash, calcium carbide, and steel slag.

Investigating the potential of IOT as a material to be incorporated into traditional earth construction techniques in regions affected by dam ruptures presents a relevant and innovative research approach. The region in which Mariana and Ouro Preto are located is connected to the origin of the occupation of Minas Gerais, and the architecture of the colonial period was widely based on earth constructions. Of the 20 buildings present in the architectural collection of the urban complex of Mariana, listed by IPHAN [42], at least 14 buildings were built with earthen techniques, with the most prevalent of them being adobe and RE. Regarding the buildings damaged by the collapse of the Fundão dam, approximately 50% were constructed using earth as a building material, employing techniques such as RE, wattle and daub, and adobe [43].

Thus, earth architecture has always been present in cities still linked to iron ore production. Furthermore, the use of IOT has not been analyzed yet in association with the earth, such that examining its characteristics to support its use in earth components remains a gap that researchers in the field of iron ore waste reuse have not filled. So, the present work aimed to characterize the tailings collected around Mariana, Barra Longa, and Rio Doce seven years after the failure of the Fundão dam.

2. Materials and Methods

In order to investigate the possible application of IOT sediments in the production of RE, the experimental design of this work was divided into three steps: (i) collection of IOT sediment and soil samples; (ii) characterization of the materials; and (iii) soil–IOT compatibility analysis for rammed earth production.

2.1. Collection/Gathering of Materials

The first step consisted of collecting IOT samples in the three municipalities in Minas Gerais that suffered the worst effect from the Fundão dam rupture: Mariana, Barra Longa, and Rio Doce (Figure 1). In Mariana, the samples (MA sample) were collected on the Gualaxo do Norte River's bank, just below the community of Bento Rodrigues, the first to be affected by the mud. The second collection was carried out in the municipality of Barra Longa (BL sample), where the mud arrived through the Gualaxo do Norte River and invaded part of this city. Part of this tailing was dredged and stored at Alta Floresta Farm, located on the river's bank, which became a surplus deposition and management area. The tailings were covered with a layer of soil for revegetation. Because of this, the samples were collected at a depth between 60 and 80 cm. The third collection point was in the Rio Doce (RD sample) municipality, where the mud reached the Carmo River (continuation of the Gualaxo do Norte) and the Risoleta Neves Hydroelectric Plant. The tailings dredged from that place were deposited at Floresta Farm, a surplus deposition and management area.

Figure 1. Location of collection points along the Rio Doce. Source: Google Maps, 2023 (modified).

All of the three IOT samples were placed in closed containers for transport. Soil samples were collected in the same region of Minas Gerais to analyze soil–IOT mixtures for RE production. Soil samples were taken from areas belonging to deposits of clayey soil, the same soil characteristic of the region where the samples were collected. This soil was chosen because of its proximity to the sediment collection site. The intention is to understand the viability of RE production with these samples once the soil–IOT geographic proximity is an important aspect of the investigation. Before the analysis, the soil and IOT samples were dried in an oven for 24 h to remove moisture, and quartered for better representation.

2.2. Materials Characterization

In the second step, the samples of IOT were analyzed by chemical, physical, and mineralogical tests to assess the sediment's characteristics, which is important to set after seven years of permanence in the environment.

The particle size of samples was analyzed using the laser granulometry test to evaluate the behavior of IOT samples in possible applications in earth components. The measurement range is from 0.04 to 2500 μm, using a laser granulometer, model Cilas 1190 Particle Size Analyzer. The specific surface and porosity analyses were performed using the Brunauer–Emmett–Teller (BET) method (adsorption of N_2 at 77 K), which consists of determining the volume of adsorbed gas from the physical adsorption isotherm, determined experimentally. The surface area was obtained from the nitrogen adsorption curve (BET method), while the distribution and pore size can be obtained from the desorption isotherm. The equipment used was a BET model Autosorb IQ Quantachrome. The unit weight and air-void content tests were also carried out according to the Brazilian technical standard NM 45 [44], the density according to the Brazilian technical standard NM 23 [45], and the water absorption according to the Brazilian technical standard NM 30 [46].

The identification and quantification of minerals and chemical components in the IOT samples were performed by X-ray fluorescence (XRF) with a WDS spectrometer, Philips PANalytical, PW-2404, with a 4 kW Rh tube. Tests were carried out to determine the inorganic constituents and evaluate the toxicity in the raw material, in addition to the analysis of the leached and solubilized extracts, in accordance with the recommendations of Brazilian technical standards 10004, 10005, and 10006 [47–49], respectively.

X-ray diffraction (XRD) analysis was performed to identify the mineral phases in the sediment samples. The equipment used was a Philips Panalytical diffractometer, system 1710. The conditions used were as follows: CuKα radiation (λ = 1.54°A), step of 0.06°/s between scanning ranges 10° to 90° at 2-theta angle (θ). The data obtained in XRD were processed using the Search Match software, version 3.1.0.2. In this software, the phases were identified, observing the characteristic diffraction patterns of each mineral and the relative intensity using the PDF-2 database of the International Center for Diffraction Data (ICDD).

The surface morphology of the IOT sediment samples was visualized by scanning electron microscopy (SEM) using a scanning electron microscope used as an FEG with FIB Nanofabrication System—Quanta FEG 3D FEI. Energy-dispersive X-ray spectrometry (EDS) was used to identify the elements present. For this, the samples were fixed on a carbon tape.

Soil samples were characterized using the Atterberg limits tests (plasticity index), XRD, XRF, and granulometry. For the determination of the soil liquidity limit, the parameters of the Brazilian NBR 6459 standard [50] were used, and the determination of the limit and the plasticity index followed the NBR 7180 [51] both with the previous drying of the samples in an oven.

In the particle size test carried out by simple sieving, it was observed that the maximum characteristic dimension was 2.40 mm and a fineness modulus of 2.90 mm. For particles smaller than 0.5 mm, laser analysis was carried out using the equipment of a particle size analyzer at the Nuclear Technology Development Center at the Federal University of Minas Gerais. The laser granulometry results showed that the soil contains 3.95% clay and silt, with 80.65% sand. According to NBR 17014 [52], the values found are lower than ideal. However, a new granulometric analysis was carried out by sedimentation, following the NBR 7181 [53] through a combination of the sieving and sedimentation methods. First, 1.5 kg of each sample was separated, passed through a 2.0 mm sieve, washed, and dried in an oven at 105 °C. After that, 70 g of the soil sample was taken for the test. The deflocculant used in this test was sodium hexametaphosphate.

2.3. Soil–IOT Compatibility Analysis

The IOT collected in Barra Longa (BL sample) was used to produce mixtures of soil–IOT, aiming to produce RE. The BL sample was chosen because of its availability and the ease of collection once this material is available to be used in any applications. Eight mixes were produced to analyze the mixture of IOT sediment and soil in the mixture for the rammed earth: one mix only with soil (reference/T0-0); three mixes with soil and IOT sediment; and four mixes with cement CP II E (Portland composite cement, like CEM-III/A [54]) and IOT sediment. Cement was used in a fixed proportion of 5% in addition to the total mass.

The cement content is related to the recommendations in the literature [55–57], which present the contents of 4% to 10% of cement as the most suitable for the stabilization of rammed earth or soil-cement blocks. Thus, it was possible to analyze mixtures with and without a binder addition. The sediment replaced the soil in groups G1 and G2. The water content varied due to the natural soil and sediment moisture and the ideal molding consistency (Table 1).

Table 1. Mixes and IOT content.

Group	Mix	Soil (%)	IOT Sediment (%)	Portland Cement (%)
G1	T0-0	100.0	-	-
	T10-0	90.0	10.0	
	T20-0	80.0	20.0	
	T40-0	60.0	40.0	
G2	T0-5	100.0	-	5.0
	T10-5	90.0	10.0	
	T20-5	80.0	20.0	
	T40-5	60.0	40.0	

The mixtures were molded in cylindrical molds with 10 cm in diameter and 20 cm in height, adapted to increase the height to obtain a greater number of layers, in a proportion of 1:2 (diameter/height). Therefore, the number of layers applied to mold the specimens was five. After preliminary analysis, 10 blows per layer were used for the correct compaction, a value adapted from NBR 7182 [58]. All layers were scarified before starting the next layer.

The metal socket was adapted from NBR 12024 [59] and NBR 7182 [58] to standardize the compaction energy. The mass of the socket was 2500 ± 10 g in a height control device of drop (guide) of 305 ± 2 mm. After weighing, the mixture was carried out in a 60 L industrial mortar mixer. Water was added gradually. After molding, the specimens were immediately demolded and placed on shelves in the open air, in a laboratory environment (open shed), under real conditions of local temperature and humidity (outdoors, only protected from rain). Specimens were not taken to chambers or greenhouses to not alter the analysis and to be as close to the curing of RE under real production conditions [60].

Six specimens were molded for each mixture, and the curing period was 28 days. At 21 days, the specimens were capped with a homogeneous mixture of cement and water to obtain smooth and uniform tops for the compressive strength test, according to NBR 12025 [61]. It was carried out with a semiautomatic hydraulic press, with a loading speed of up to 1.00 KN/min. The analysis of results was based on the Brazilian technical standard NBR 7215 [62]. The average of the individual strength values of the specimens was calculated in MPa. After finding an average, it was necessary to calculate the maximum relative deviation (MRD). When it is greater than 6%, it is necessary to calculate a new average, disregarding the outlier and persisting the calculated value until reaching the MRD value ≤ 6% [62].

3. Results

3.1. IOT Sample Characterization and Analysis

Here in this item are the results of the sample characterization test. Figure 2 shows the granulometric curves of the IOT samples from Mariana (MA sample), Rio Doce (RD Sample), and Barra Longa (BL Sample).

Through the curves obtained, it is possible to observe that both samples have sandy characteristics with an insignificant portion of clay. According to Figueiredo et al. [27], this fact is associated with the composition of the tailings from the Fundão Dam, which was a mixture of sandy tailings and mud. The diameters varied between 1 and 200 µm, with greater predominance in a range close to 15 µm and 100 µm. Such values are consistent with those obtained in other works of characterization of the tailings from the rupture of the Fundão dam carried out by other authors [24,25,27].

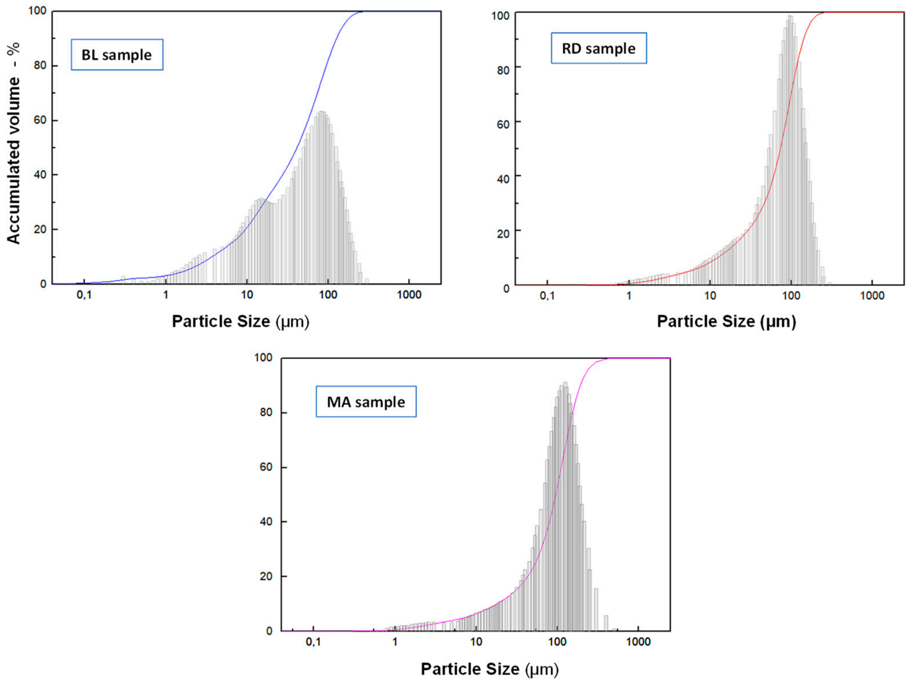

Figure 2. Granulometric curves of tailing samples.

Figure 3 shows the isotherm curves of the tailing's samples, obtained by the analysis of nitrogen adsorption and desorption. According to other works found in the literature, the isotherms obtained have a type II profile. According to IUPAC (International Union of Pure and Applied Chemistry), these curves are characteristics of nonporous or macroporous materials [63].

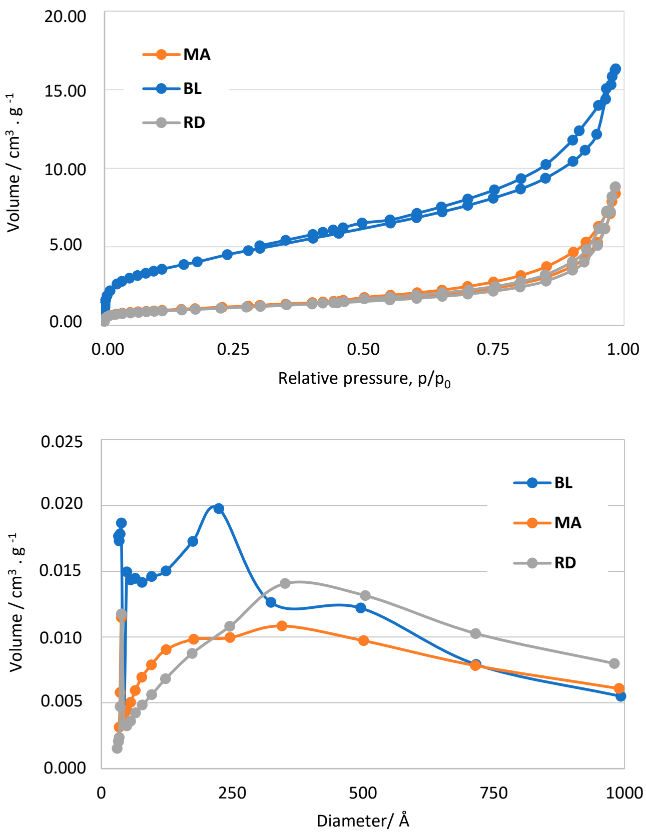

Figure 3. N_2 sorption isotherms for the tailing's samples.

It is possible to see the presence of narrow and inclined hysteresis, classified as H3 type, indicative of nonrigid aggregates of lamellar particles, mainly mesopores/macropores in the form of slits or parallel plates [64,65]. Table 2 presents the specific surface area and porosimetry, and it is possible to observe that all of the samples are similar regarding the pore volume and diameter values. As expected for this type of sample, the specific surface area values were low and similar. Such results are compatible with other studies carried out with ore tailings. Almeida et al. [25] found specific surface area (SSA) and silt and clay size values of 5.25, 5.66, and 20.77 $m^2\ g^{-1}$, respectively.

Table 2. Specific surface area and porosimetry of sedimented tailings samples.

Samples	Specific Surface Area (m^2/g)	Pore Volume (cm^3/g)	Pore Diameter (mm)
MA Sample	3.60	0.013	3.864
RD Sample	3.26	0.013	3.873
BL Sample	7.28	0.020	3.300

Table 3 shows the results obtained for the specific mass, unit mass, void index, and water absorption tests. Comparing the specific mass values found with the other results [66,67] it is possible to attest that they are compatible with silica-rich tailings with lower concentrations of iron due to the density closest to sand, which is 2.65 g/cm^3. These results are consistent with those found in the mineralogical analysis, which showed quartz as the most present mineral in the samples, directly interfering with the specific mass results. The values obtained for the void ratio were similar. Relating to the characteristic granulometry of iron ore tailings, which presents a high concentration of particles of the same size, representing a uniform granulometric curve, a relatively high void volume index might be expected.

Table 3. Specific mass, unit mass, void index, and water absorption of tailings samples.

Samples	Physical Tests			
	Specific Mass (g/cm^3)	Unit Mass (kg/m^3)	Void Index (%)	Water Absorption (%)
MA Sample	2.93	1526.50	66.9	2.97
RD Sample	2.82	1498.70	64.5	3.33
BL Sample	2.79	1368.47	64.2	7.52

The values obtained for the water absorption test showed that the tailings from Mariana (MA sample) and Rio Doce (RD sample) have a low rate of water absorption, which is expected for tailings composed mainly of silica. The Barra Longa tailings (BL sample) showed a higher water absorption rate than the other samples, which may be related to clay minerals in the sample. Additionally, the BL sample showed a lower value of specific mass, which attests to the higher presence of clay minerals in the sample. According to Taiz et al. [68], clayey soils retain a higher water content than sandy soils due to the larger surface area and smaller pores between particles, which can be confirmed by the specific surface area results obtained and shown in Table 2.

Table 4 presents the results obtained from the XRF analyses. The oxides found in the samples match the mineralogical phases obtained by XRD. Furthermore, among the oxides found in the tailings samples, the highest concentrations are quartz (SiO_2) and hematite (α-Fe_2O_3). According to other authors [28,69], quartz and hematite are the main mineral components of tailings from the Fundão dam. Traces of manganese oxide, zinc, chromium, and sodium were also found.

Table 4. Chemical analysis of samples by X-ray fluorescence.

Samples	Chemical Composition (%)									
	SiO_2	Fe_2O_3	Al_2O_3	TiO_2	K_2O	MnO	CaO	P_2O_5	MgO	Na_2O
MA Sample	78.13	8.88	1.09	0.21	0.20	0.28	0.04	0.007	<0.10	<0.10
RD Sample	76.85	8.46	2.49	0.27	0.34	0.05	0.24	0.010	<0.10	<0.10
BL Sample	67.05	9.57	6.39	0.67	0.62	0.07	0.21	0.022	<0.10	<0.10

Due to the possibility of contamination of these samples in the environment, since the rivers Gualaxo do Norte, Carmo, and Doce have been used, over the decades, for gold mining during the colonial period in Brazil, assays for the determination of inorganic constituents in the raw material, in addition to analysis of the leached and solubilized extracts, are shown to be extremely important. The possibility of contamination was raised at the time of the accident [8,24,70] but after five years, the pollutant load of these rivers may have been concentrated or dispersed, which may have impacted on the composition of these sediments.

Through the data obtained by the tests of determination of heavy metals in raw material and obtaining of leached and solubilized extracts, it was observed that the raw material and the leaching of metals (inorganic) presented results with values below the maximum limits prescribed by the NBR 10004 standard [47]. The leaching and solubilization tests of volatile and semivolatile organics also showed null results, i.e., below the detection limits of the technique adopted and below the maximum limits prescribed by NBR 10004 [47].

However, iron, aluminum, lead (only in the MA sample), and manganese (only in the BL sample) showed values above the limit recommended by NBR 10004. Alumina and iron presented values 12–20 times higher and 40 times higher, respectively, than the accepted limit. Because of that, the data indicate that all the collected tailings samples can be classified as Class II A—non-hazardous non-inert [47].

A radioactivity analysis of the samples was not carried out. Still, a study with Candonga tailings (collected after the Fundao Dam collapse) and Itabirite waste (collected in the dam) was carried out in 2017. It was concluded that the radionuclide content of the samples, even after some mixture with clay material, is very low, and even much lower than conventional materials used in civil construction (natural sand and cement) [71].

The X-ray diffractograms obtained from the tailing's samples can be seen in Figure 4. It was possible to observe the great similarity between the diffractograms of the analyzed samples, with a predominant presence of Quartz phases, SiO_2 (ICDD—46-1045); Hematite, α—Fe_2O_3 (ICDD—33-664); Goethite, α—FeO(OH) (ICDD—74-2195); and Kaolinite, $Al_2Si2O_5(OH)_4$ (ICDD—80-885). Although the intensity of the peaks of each mineral does not represent the amount, it can indicate which mineral is probably present in the sample.

This result is consistent with those found in the literature [25,28,66,72–74] confirming the results obtained in the X-ray fluorescence analysis. XRD analysis also allows one to evaluate the amorphicity of the samples, which would make this material suitable for use as a pozzolanic mineral addition, which would increase the durability of cementitious matrices [75] or as a precursor in alkali-activated materials [19,22,76]. A crystalline material, as shown in the tailing's samples, however, may have its reactivity improved through grinding and calcination [77–79] depending on its use.

The images obtained through scanning electron microscopy (SEM) analysis may be seen in Figure 5. Through the images, it was possible to observe that the particle size is compatible with the results obtained by laser granulometry, with a maximum diameter close to 200 μm. These results agree with other researchers [24,25] who found these same characteristics for tailings from the Fundão dam failure.

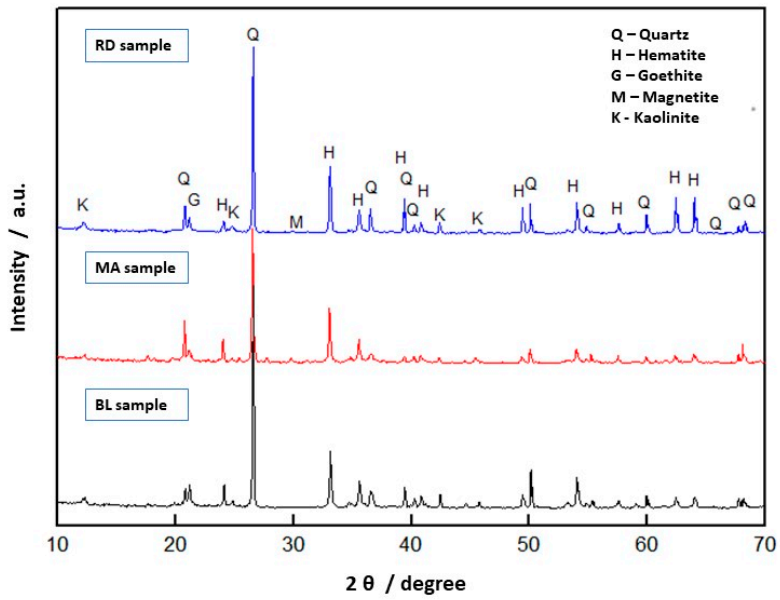

Figure 4. X-ray diffractograms of the tailing's samples.

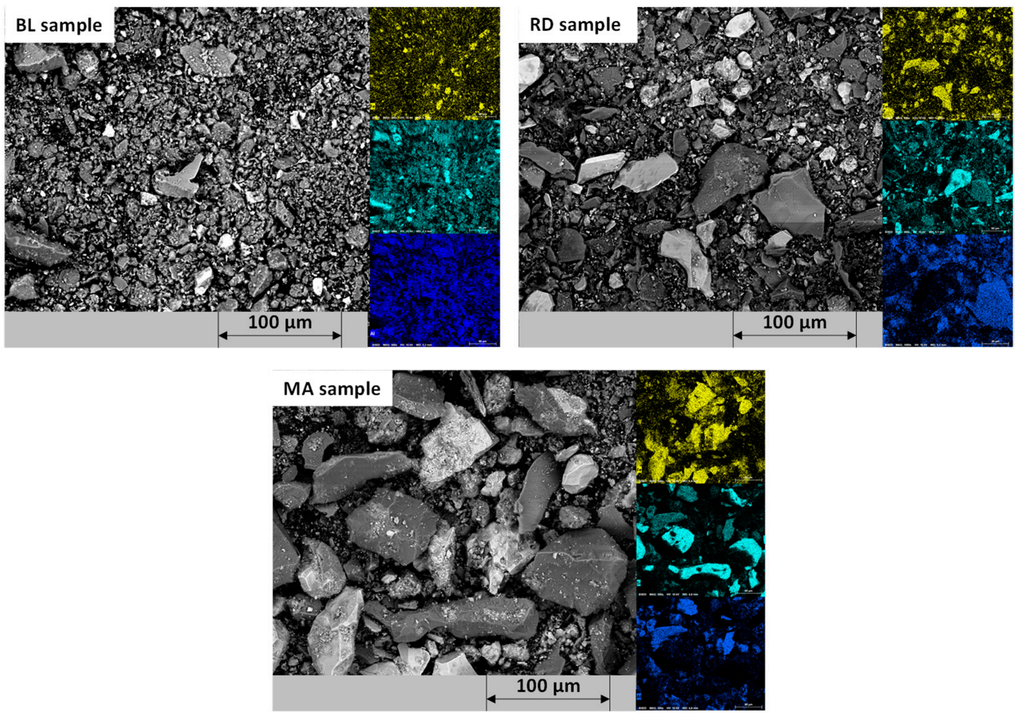

Figure 5. Scanning electron microscopy images of tailing's samples.

It is also possible to identify the presence of prismatic particles with sharp edges, presenting edges and vertices, and the presence of tabular and granular particles. According to Shettima et al. [12] and Zhao et al. [80], the particles of the first type may be associated with quartz particles. Particles of the second type may indicate the presence of hematite particles [72,75]. According to Dedavid et al. [81], the contrast of the images is related to the atomic number of the elements present in the sample. Thus, through the images obtained, it can be affirmed that quartz particles have larger granulometry when compared to ferrous mineral particles.

In the images generated for the samples from Rio Doce and Mariana, it is possible to observe particles with rough and angular surfaces, which is expected for a material obtained during mineral processing, with comminution steps [27]. In the BL sample, it was possible to perceive a smaller number of particles of ferrous minerals, represented by the light-gray color. This can also be seen with the help of EDS images. It also shows predominantly dark-colored particles characteristic of quartz.

In general, the tailing samples were similar. Traditionally, however, Brazilian IOT, collected in dams, still has a high amount of iron [72,75] due to the still inefficient extraction processes practiced 30–40 years ago. Through the characterization, it can be observed that this material, when exposed to the weather, underwent significant changes over time. Even so, it is a material stored for future use, as its permanence in the places where it is found changes the landscapes, the soil, and the waters, as reported by Brazilian researchers in postaccident publications [8,28,29,69,82].

3.2. Soil–IOT Compatibility to Produce RE

Table 5 shows the soil samples' characteristics. It was found that the clay contents and sand were quite different, with soil with a high clay content and fine particles. In this way, the need to correct the soil with the IOT-S became even more evident.

Table 5. Soil characterization.

Specific mass (kg/m^3)	2340	Liquidity limit	53
Unit mass (kg/m^3)	1012	Plasticity limit	31
Volume of voids (%)	57.50	Plasticity index	22
Granulometry (%)			
Clay	55.5	Silt	14.5
Sand	28.0	Gravel	2.0
Average diameter (μm)	26.4		

As it was carried out before the launch of the Brazilian rammed earth standard [52], the results of the physical characterization of the soil were based on the parameters of the soil-cement standards and adobe, as well as recommendations from the scientific literature, which determine values between 35% and 45% for the liquidity limit and between 7% and 30% for the plasticity index [83]. In this sense, the results demonstrate that the soil analysis could benefit from stabilization since its value for the liquidity limit exceeds the recommendation.

The results of the compressive strength test are presented in Table 6. From the values obtained, it is possible to infer that the addition of 5% cement to the soil and the stabilization with IOT proved to be adequate in comparison to the reference values (T0-0), which do not have the addition of any component. For the mixtures without the addition of cement, only with IOT, it was observed that the compressive strength values increase as there is an increase in the replacement of soil by sedimented tailing, in proportions of 10%, 20%, and 40%.

Table 6. Compressive strength—Soil–IOT samples.

Mixture	Compressive Strength (MPa)	Standard Deviation	Coefficient of Variation (%)
T0-0	0.72	0.08	11.55
T10-0	1.12	0.13	11.90
T20-0	1.24	0.05	4.07
T40-0	1.80	0.15	8.53
T0-5	1.35	0.14	10.63
T10-5	1.07	0.11	9.91
T20-5	1.27	0.15	12.20
T40-5	1.57	0.08	4.98

Regarding the compressive strength values found in the literature, it is important to say that the reference trace (T0-0), only with unstabilized soil, is outside the parameters of what is considered satisfactory for RE, while the values of samples stabilized with IOT are within the recommended range. The adopted values range from 1.0 MPa to 2.0 MPa [60,83] for the compressive strength of RE and earth constructions. In other research [84], the results were between 1.0 and 2.5 MPa, consistent with the present study. With the addition of cement, Eusébio [85] used a content of 7% of the stabilizing material and obtained a compressive strength greater than 2.0 MPa. Jayasinghe and Kamaladasa [86] analyzed the compressive strength of RE walls stabilized with cement contents in the range of 6.8 and 10%, and observed that the stabilizing action of cement is more effective for sandy soils. However, they still obtained high resistance values for clayey soils.

It is important to point out that the highest values obtained were for the mix with the highest amount of IOT (T40-0), which reached 1.80 MPa, followed by the mix with IOT and cement (T40-5). Because of that, there is a tendency to adequately stabilize with only IOT, without the addition of cement, which has been more effective, especially at higher levels of IOT addition (40%).

Finally, the Peruvian technical standard E.080 [87] and the NZS 4297 standard [88] present values of 1.0 MPa and 0.50 MPa, respectively, for RE compressive strength. In other words, the results found in this research are superior to the recommendations, including the Brazilian standard [52], even though this study was developed before its launch.

4. Discussion

Characterizing iron mining waste disposed in the environment is of fundamental importance for its correct use and recovery. The analysis carried out with samples of tailings from the three cities most impacted by the accident made it possible to see that the IOT is a crystalline material with a high silica content. Even after being mixed with the local environment, the tailings collected still have a high content of iron, when compared to the soil itself. The quartz content and specific surface area/grain size vary depending on the collection site. Due to the high availability of this material, correct and up-to-date analysis can make the application easier and more viable.

The compressive strength initial results indicate the possibility of using this material as a physical stabilizer to produce earthen components, notably the RE, without cement or lime addition, which may contribute to less environmental impact. As the RE needs a sandy mixture to have better mechanical behavior, the use of tailings is a prominent strategy to reduce the cement's use, and, additionally, the embodied energy of the technique when applied in mining areas.

Furthermore, since the samples collected were classified as non-hazardous materials, IOT can be used by communities to reconstruct their buildings without eliminating the vernacular techniques known by them. Using IOT as an inert material to produce traditional earthen constructions can be also aligned with social sustainability and innovation of the earth's construction techniques. The study showed a positive interaction between a clayey soil and the IOT collected in the Rio Doce region. This is probably due to the rocky origin common to both materials. The advantages can be seen, especially concerning the compressive strength of the RE stabilized with IOT, without cement, compared to the RE cylindrical specimens without any stabilization.

Cost analyses were not carried out as they were not included in the scope of this work. Nevertheless, the cost reduction may be observed once the IOT samples can be used as construction material within the communities surrounded by the Rio Doce basin.

Notably, IOT is a waste with a high capacity to be incorporated into civil construction, without associated environmental risks. This research has shown that the same IOT can be incorporated into traditional, vernacular construction techniques, in balance with the memory and way of building traditional communities. Proving the compatibility of IOT with a construction technique that is ancient, but which remains a major bet in the search for a lower-impact construction can help solve two major problems related to the sustainability of construction: tailings disposal and carbon generation.

5. Conclusions

The main conclusions obtained by this research are listed as follows:

(a) The tailings collected in the Rio Doce basin, 7 years after the disaster with Fundao Dam, are crystalline and with a high content of silica.
(b) The samples collected in the Rio Doce basin may be classified as Class II A—non-hazardous non-inert, once some of them presented heavy metals content above the limit established by NBR 10004 (solubilized extract),
(c) The analysis of heavy metals on the raw samples did not indicate the presence of organic or inorganic metals, which means that they may be used by the communities as a construction material.
(d) The cylindrical specimens of RE, produced only with soil and IOT, showed compressive strength values above international standards, which may indicate the innovative viability of using IOT as a physical stabilizer for earthen construction.

Author Contributions: Conceptualization, S.B. and M.T.A.; methodology, S.B., M.T.A., F.L., R.L. and A.P.T.; investigation, M.D., G.L., I.M., R.G., R.L., F.L. and A.P.T.; writing—original draft preparation, S.B., G.L. and M.D.; writing—review and editing, S.B. and M.T.A.; visualization, M.T.A.; project administration, S.B. All authors have read and agreed to the published version of the manuscript.

Funding: This research was funded by Minas Gerais State Research Foundation—FAPEMIG [process APQ05495-18]; by the National Council for Scientific and Technological Development (CNPq); and by the Brazilian Federal Agency for Support and Evaluation of Graduate Education (Coordenação de Aperfeiçoamento de Pessoal de Nível Superior—CAPES), for their financial support in scientific initiation and master's degree scholarships (Finance Code 001).

Data Availability Statement: Data on which this paper is based are available from the authors upon reasonable request. The data are not publicly available due to the privacy.

Acknowledgments: The authors would like to express their gratitude to the Renova Foundation.

Conflicts of Interest: The authors declare no conflicts of interest.

References

1. U.S. Geological Survey. *Mineral Commodity Summaries*; U.S. Geological Survey: Reston, VA, USA, 2020; p. 89.
2. IBRAM—Instituto Brasileiro de Mineração. Riscos e Oportunidades de Negócios em Mineração e Metais no Brasil. 2021. Available online: https://ibram.org.br/wp-content/uploads/2021/04/Estudo-Mineracao-e-Metais_EY-e-IBRAM_Versao-050421.pdf (accessed on 2 November 2021). (In Portuguese).
3. IPT—Instituto de Pesquisas Tecnológicas. Rejeitos de Mineração. Available online: http://www.ipt.br/noticias_interna.php?id_noticia=1043%3E (accessed on 11 June 2021). (In Portuguese).
4. IPEA—Instituto de Pesquisa e Economia Aplicada. Diagnóstico dos Resíduos Sólidos da Atividade de Mineração de Substâncias Não-Energéticas. Available online: https://repositorio.ipea.gov.br/bitstream/11058/7702/1/RP_Diagn%C3%B3stico_2012.pdf (accessed on 2 November 2021).
5. ANM—Agência Nacional de Mineração. Classificação de Barragens de Mineração. 2020. Available online: http://www.anm.gov.br/assuntos/barragens/plano-de-seguranca-de-barragens (accessed on 2 November 2021).
6. O TEMPO. Vale Começa Obra Para Descaracterizar Mais Uma Barragem a Montante em MG. O TEMPO, 17 March 2023. Available online: https://encurtador.com.br/gEHO8 (accessed on 25 April 2023).
7. Lacaz, F.A.C.; Porto, M.F.S.; Pinheiro, T.M.M. Tragédias brasileiras contemporâneas: O caso do rompimento da barragem de rejeitos de Fundão/Samarco. *Rev. Bras. Saúde Ocup.* **2017**, *42*, e9. [CrossRef]
8. Gomes, L.E.O.; Correa, L.B.; Sa, F.; Neto, R.R.; Bernardino, A.F. The impacts of the Samarco mine tailing spill on the Rio Doce estuary, Eastern Brazil. *Mar. Pollut. Bull.* **2017**, *120*, 28–36. [CrossRef] [PubMed]
9. Fundação Renova. Retomada das Atividades na Fazenda Floresta. Available online: https://www.fundacaorenova.org/noticia/retomada-das-atividades-na-fazenda-floresta/ (accessed on 5 November 2021).
10. Assis, D.M.; Queiroga, F.O.C.S.; Mendes, J.C. Utilização de rejeito de barragem de minério de ferro na fabricação de tijolos maciços. *A Rev. Científ. FaSaR* **2018**, *3*, 191–200.
11. Carrasco, E.V.M.; Magalhaes, M.D.C.; Santos, W.J.D.; Alves, R.C.; Mantilla, J.N.R. Characterization of mortars with iron ore tailings using destructive and nondestructive tests. *Constr. Build. Mater.* **2017**, *131*, 31–38. [CrossRef]

12. Shettima, A.U.; Hussin, M.W.; Ahmad, Y.; Mirza, J. Evaluation of iron ore tailings as replacement for fine aggregate in concrete. *Constr. Build. Mater.* **2016**, *120*, 72–79. [CrossRef]
13. Yunhong, C.; Fei, H.; Wenchuan, L.; Rui, L.; Guanglu, L.; Jingming, W. Test research on the effects of mechanochemically activated iron tailings on the compressive strength of concrete. *Constr. Build. Mater.* **2016**, *118*, 164–170. [CrossRef]
14. Morais, C.F.; Belo, B.R.; Bezerra, A.C.S.; Loura, R.M.; Porto, M.P.; Bessa, S.A.L. Thermal and mechanical analyses of colored mortars produced using Brazilian iron ore tailings. *Constr. Build. Mater.* **2021**, *268*, 121073. [CrossRef]
15. Galvão, J.L.B.; Andrade, H.D.; Brigolini, G.J.; Peixoto, R.A.F.; Mendes, J.C. Reuse of iron ore tailings from tailings dams as pigment for sustainable paints. *J. Clean. Prod.* **2018**, *200*, 412–422. [CrossRef]
16. Li, R.; Zhou, Y.; Li, C.; Li, S.; Huang, Z. Recycling of industrial waste iron tailings in porous bricks with low thermal conductivity. *Constr. Build. Mater.* **2019**, *213*, 43–50. [CrossRef]
17. Mendes, B.C.; Pedroti, L.G.; Fontes, M.P.F.; Ribeiro, J.C.L.; Vieira, C.M.F.; Pacheco, A.A.; Azevedo, A.R.G. Technical and environmental assessment of the incorporation of iron ore tailings in construction clay bricks. *Constr. Build. Mater.* **2019**, *227*, 116669. [CrossRef]
18. Bessa, S.A.L.; Miranda, M.A.; Arruda, E.A.M.; Bezerra, A.C.S.; Sacht, H.M. Produção e avaliação de microconcretos com rejeito de minério de ferro para a fabricação de componentes construtivos. *Mater. Rio De Jan.* **2022**, *27*, 1–14. (In Portuguese) [CrossRef]
19. Defáveri, K.C.S.; Santos, L.F.; Carvalho, J.M.F.; Peixoto, R.A.F.; Silva, G.J.B. Iron ore tailing-based geopolymer containing glass wool residue: A study of mechanical and microstructural properties. *Constr. Build. Mater.* **2019**, *220*, 375–385. [CrossRef]
20. Duan, P.; Yan, C.; Zhou, W.; Ren, D. Development of fly ash and iron ore tailing based porous geopolymer for removal of Cu (II) from wastewater. *Ceram. Int.* **2016**, *42*, 13507–13518. [CrossRef]
21. Kuranchie, F.A.; Shukla, S.K.; Habibi, D. Utilization of iron ore mine tailings for the production of geopolymer bricks. *Int. J. Min. Reclam. Environ.* **2016**, *30*, 92–114. [CrossRef]
22. Obenaus-Emler, R.; Falah, M.; Illikainen, M. Assessment of mine tailings as precursors for alkali-activated materials for on-site applications. *Constr. Build. Mater.* **2020**, *246*, 118470. [CrossRef]
23. Lage, G.T.L.; Vimieiro, J.I.C.; Matias, L.M.; Costa, J.M.; Batista, G.E.F.; Bessa, S.A.L. Caracterização do sedimento de rejeito de minério de ferro para uso como estabilizante da taipa de pilão. In Proceedings of the 4º Congresso Luso-Brasileiro de Materiais de Construção Sustentáveis, Salvador, Bahia, Brasil, 9–11 November 2022; pp. 620–633. (In Portuguese).
24. Segura, F.R.; Nunes, E.A.; Paniz, F.P.; Paulelli, A.C.C.; Rodrigues, G.B.; Braga, G.U.L.; Pedreira, W.D.; Barbosa, F.; Cerchiaro, G.; Silva, F.F.; et al. Potential risks of the residue from Samarco's mine dam burst (Bento Rodrigues, Brazil). *Environ. Pollut.* **2016**, *218*, 813–825. [CrossRef] [PubMed]
25. Almeida, C.A.; Oliveira, A.F.; Pacheco, A.A.; Lopes, R.P.; Neves, A.A.; Queiroza, M.E.L.R. Characterization and evaluation of sorption potential of the iron mine waste after Samarco dam disaster in Doce River basin—Brazil. *Chemosphere* **2018**, *209*, 411–420. [CrossRef]
26. Machado, M.S.M.M.; Santos, A.M.M.; Freire, C.B.; Guimarães, A.C.P.D.; Lameiras, F.S. Blocks for civil construction made with the sediment deposited in the Candonga Dam. *Metall. Mater.* **2019**, *72*, 5–111. [CrossRef]
27. Figueiredo, M.D.; Lameiras, F.S.; Ardisson, J.D.; Araújo, M.H.; Texeira, A.P.C. Tailings from Fundão Tragedy: Physical–Chemical Properties of the Material That Remains by Candonga Dam. *Integr. Environ. Assess. Manag.* **2020**, *16*, 636–642. [CrossRef]
28. Couto, F.R.; Ferreira, A.M.; Pontes, P.P.; Marques, A.R. Physical, Chemical and Microbiological Characterization of the Soils Contaminated by Iron Ore Tailing Mud After Fundão Dam Disaster in Brazil. *Appl. Soil Ecol.* **2021**, *158*, 103811. [CrossRef]
29. Duarte, E.B.; Neves, M.A.; de Oliveira, F.B.; Martins, M.E.; de Oliveira, C.H.R.; Burak, D.L.; Orlando, M.T.D.; Rangel, C.V.G.T. Trace metals in Rio Doce sediments before and after the collapse of the Fundão iron ore tailing dam, Southeastern Brazil. *Chemosphere* **2021**, *262*, 127879. [CrossRef] [PubMed]
30. Minke, G. *Manual de Construção com Terra: Uma Arquitetura Sustentável*; B4 Editores: São Paulo, Brasil, 2015; 225p. (In Portuguese)
31. Arrigoni, A.; Grillet, A.C.; Pelosato, R.; Dotelli, G.; Beckett, C.T.S.; Woloszyn, M.; Ciancio, D. Reduction of rammed earth's hygroscopic performance under stabilization: An experimental investigation. *Build. Environ.* **2017**, *115*, 358–367. [CrossRef]
32. Hoffmann, M.V.; Minto, F.C.N.; Heise, A.F. Taipa de Pilão. In *Técnicas de Construção com Terra*; Neves, C., Faria, O.B., Eds.; FEB-UNESP/PROTERRA: Bauru, Brasil, 2011; pp. 46–60. (In Portuguese)
33. Da Rocha, C.G.; Consoli, N.C.; dalla Rosa Johann, A. Greening stabilized rammed earth: Devising more sustainable dosages based on strength controlling equations. *J. Clean. Prod.* **2014**, *66*, 19–26. [CrossRef]
34. Siddiqua, S.; Barreto, P.N.M. Chemical stabilization of rammed earth using calcium carbide residue and fly ash. *Constr. Build. Mater.* **2018**, *169*, 364–371. [CrossRef]
35. Munoz, P.; Letelier, V.; Munoz, L.; Bustamante, M.A. Adobe bricks reinforced with paper e pulp wastes improving thermal and mechanical properties. *Constr. Build. Mater.* **2020**, *254*, 119314. [CrossRef]
36. Olacia, E.; Pisello, A.L.; Chiodo, V.; Maisano, S.; Frazzica, A.; Cabeza, L.F. Sustainable adobe bricks with seagrass fibres. Mechanical and thermal properties characterization. *Constr. Build. Mater.* **2020**, *239*, 117669. [CrossRef]
37. Meek, A.H.; Beckett, C.T.S.; Elchalakani, M. Reinforcement corrosion in cement and alternatively stabilised rammed earth materials. *Constr. Build. Mater.* **2021**, *274*, 122045. [CrossRef]
38. Kariyawasam, K.K.G.K.D.; Jayasinghe, C. Cement stabilized rammed earth as a sustainable construction material. *Constr. Build. Mater.* **2016**, *105*, 519–527. [CrossRef]

39. Venkatarama Reddy, B.; Leuzinger, G.; Sreeram, V.S. Low embodied energy cement stabilised rammed earth building—A case study. *Energy Build.* **2014**, *68*, 541–546. [CrossRef]
40. Kosarimovahhed, M.; Toufigh, V. Sustainable usage of waste materials as stabilizer in rammed earth structures. *J. Clean. Prod.* **2020**, *277*, 123279. [CrossRef]
41. Giuffrida, G.; Caponetto, R.; Cuomo, M. An overview on contemporary rammed earth buildings: Technological advances in production, construction, and material characterization. In *Earth and Environmental Science*; IOP Conference Series; Institute of Physics Publishing: Bristol, UK, 2019.
42. IPHAN. *Inventário Nacional de Bens Imóveis e Sítios URBANOS Tombados*; E-book; IPHAN: Brasília, Brasil, 2007; Volume 82, Available online: https://livraria.senado.leg.br/inventarionacional-de-bens-imoveis-e-sitios-urbanos-tombados-vol-82. (accessed on 22 January 2023).
43. Lage, G.T.L.; Nogueira, J.A.W.; Saraiva, S.H.M.; Bessa, S.A.L. Arquitetura de terra em regiões afetadas pelo rompimento da barragem de Fundão. In Proceedings of the TerraBrasil 2022—Congresso de Arquitetura e Construção com Terra no Brasil, Campus da Universidade Federal de Santa Catarina—UFSC, Florianópolis, Brasil, 28 January 2022; pp. 232–244. (In Portuguese).
44. ABNT—Associação Brasileira de Normas Técnicas. *NBR NM 45: Aggregates—Determination of the Unit Weight and Air-Void Contends*; ABNT: Rio de Janeiro, Brasil, 2006. (In Portuguese)
45. ABNT—Associação Brasileira de Normas Técnicas. *NBR NM 23: Portland Cement and Other Powdered Materials—Determination of Specific Gravity*; ABNT: Rio de Janeiro, Brasil, 2000. (In Portuguese)
46. ABNT—Associação Brasileira de Normas Técnicas. *NBR NM 30: Fine Aggregate—Test Method for Water Absorption*; ABNT: Rio de Janeiro, Brasil, 2000. (In Portuguese)
47. ABNT—Associação Brasileira de Normas Técnicas. *NBR 10004: Solid Waste—Classification*; ABNT: Rio de Janeiro, Brasil, 2004. (In Portuguese)
48. ABNT—Associação Brasileira de Normas Técnicas. *NBR 10005: Procedure for Obtention Leaching Extract of Solid Wastes*; ABNT: Rio de Janeiro, Brasil, 2004. (In Portuguese)
49. ABNT—Associação Brasileira de Normas Técnicas. *NBR 10006: Procedure for Obtention of Solubilized Extraction of Solid Wastes*; ABNT: Rio de Janeiro, Brasil, 2004. (In Portuguese)
50. ABNT—Associação Brasileira de Normas Técnicas. *NBR 6459: Solo—Determinação do Limite de Liquidez*; ABNT: Rio de Janeiro, Brasil, 2016. (In Portuguese)
51. ABNT—Associação Brasileira de Normas Técnicas. *NBR 7180: Solo—Determinação do Limite de Plasticidade*; ABNT: Rio de Janeiro, Brasil, 2016. (In Portuguese)
52. ABNT—Associação Brasileira de Normas Técnicas. *NBR 17014: Taipa de Pilão: Requisitos, Procedimentos e Controle*; ABNT: Rio de Janeiro, Brasil, 2022. (In Portuguese)
53. ABNT—Associação Brasileira de Normas Técnicas. *NBR 7181: Solo—Análise Granulométrica*; ABNT: Rio de Janeiro, Brasil, 2018. (In Portuguese)
54. *British Standard: EN 197-1*; Cement Composition, Specifications and Conformity Criteria for Common Cements. European Committee for Standardization: Brussels, Belgium, 2011.
55. Guettala, A.; Abibsi, A.; Houari, H. Durability study of stabilized earth concrete under both laboratory and climatic conditions exposure. *Constr. Build. Mater.* **2006**, *20*, 119–127. [CrossRef]
56. Gramlich, A.N. A Concise History of the Use of the Rammed Earth Building Technique Including Information on Methods of Preservation, Repair, and Maintenance. Master's Thesis, University of Oregon, Eugene, OR, USA, 2013.
57. Khadka, B. Rammed earth, as a sustainable and structurally safe green building: A housing solution in the era of global warming and climate change. *Asian J. Civ. Eng.* **2020**, *21*, 119–136. [CrossRef]
58. ABNT—Associação Brasileira de Normas Técnicas. *NBR 7182: Solo—Ensaio de Compactação*; ABNT: Rio de Janeiro, Brasil, 2022. (In Portuguese)
59. ABNT—Associação Brasileira de Normas Técnicas. *NBR 12024: Solo-Cimento—Moldagem e Cura de Corpos-de-Prova Cilíndricos—Procedimento*; ABNT: Rio de Janeiro, Brasil, 2012. (In Portuguese)
60. Ciancio, D.; Jaquin, P.; Walker, P. Advances on the assessment of soil suitability for rammed earth. *Constr. Build. Mater.* **2013**, *42*, 40–47. [CrossRef]
61. ABNT—Associação Brasileira de Normas Técnicas. *NBR 12025: Solo-Cimento—Ensaio de Compressão Simples de Corpos de Prova Cilíndricos—Método de Ensaio*; ABNT: Rio de Janeiro, Brasil, 2012. (In Portuguese)
62. ABNT—Associação Brasileira de Normas Técnicas. *NBR 7215: Cimento Portland—Determinação da Resistência à Compressão de Corpos de Prova Cilíndricos*; ABNT: Rio de Janeiro, Brasil, 2019. (In Portuguese)
63. Thommes, M.; Kaneko, K.; Neimark, A.V.; Olivier, J.P.; Rodriguez-Reinoso, F.; Rouquerol, J.; Sing, K.S.W. Physisorption of gases, with special reference to the evaluation of surface area and pore size distribution (IUPAC Technical Report). *Pure Appl. Chem.* **2015**, *87*, 1051. [CrossRef]
64. Pena, E.Q.; Vieira, C.B.; Silva, C.A.; Seshadri, V.; Araújo, F.G.S. Caracterização de parâmetros de porosidade de concentrados de minérios de ferro pelo método de adsorção de nitrogênio. *Tecnol. Em Metal. E Mater.* **2008**, *4*, 53–57. [CrossRef]
65. Sing, K.S.W.; Everett, D.H.; Haul, R.A.W.; Moscou, L.; Pierotti, R.A.; Rouquérol, J.; Siemieniewska, T. Reporting physisorption data for gas/solid systems with special reference to the determination of surface area and porosity. *Pure Appl. Chem.* **1985**, *57*, 603–619. [CrossRef]

66. Fontes, W.C.; Mendes, J.C.; Silva, S.N.; Peixoto, R.A.F. Mortars for laying and coating produced with iron ore tailings from tailing dams. *Constr. Build. Mater.* **2016**, *112*, 988–995. [CrossRef]
67. Silva, R.A.; Soares, E.; Oliveira, D.V.; Miranda, T.; Cristelo, N.M.; Leitão, D. Mechanical characterisation of dry-stack masonry made of CEBs stabilised with alkaline activation. *Constr. Build. Mater.* **2015**, *75*, 349–358. [CrossRef]
68. Taiz, L.; Zeiger, E. *Plant Physiology*; The Benjamim/Cummings Publishing Company, Inc.: Redwood City, CA, USA, 1991.
69. Orlando, M.T.D.; Galvão, E.S.; Cavichini, A.S.; Rangel, C.V.G.T.R.; Orlando, C.G.P.; Grilo, C.F.; Soares, J.; Oliveira, K.S.S.; SÁ, F.; Junior, A.C.; et al. Tracing iron ore tailings in the marine environment: An investigation of the Fundão dam failure. *Chemosphere* **2020**, *257*, 127184. [CrossRef]
70. Hatje, V.; Pedreira, R.M.A.; Rezende, C.E.; Schettini, C.A.F.; Souza, G.C.; Marin, D.C.; Hackspacher, P.C. The environmental impacts of one of the largest tailing dam failures worldwide. *Sci. Rep.* **2017**, *7*, 10706. [CrossRef]
71. Freire, C.B.; Santos, T.; Sales, G.; Lameiras, F.; Rocha, Z.; Cuccia, V. Radioactivity assessment of the waste deposited in Candonga's lake after the Fundão dam's collapse. *Braz. J. Radiat. Sci.* **2019**, *7*, 1–13. [CrossRef]
72. Dauce, P.D.; Castro, G.B.; Lima, M.M.F.; Lima, R.M.F. Characterization and magnetic concentration of an iron ore tailings. *J. Mater. Res. Technol.* **2019**, *8*, 1052–1059. [CrossRef]
73. De Andrade, L.C.R. Caracterização de Rejeitos de Mineração de Ferro, in Natura e Segregados, para Aplicação como Material de Construção Civil. Ph.D. Thesis, Universidade Federal de Viçosa, Viçosa, Brasil, 2014. (In Portuguese).
74. Bastos, L.A.C.; Silva, G.C.; Mendes, J.C.; Peixoto, R.A.F. Using Iron Ore Tailings from Tailing Dams as Road Material. *J. Mater. Civ. Eng.* **2016**, *28*, 04016102. [CrossRef]
75. Zhang, N.; Tang, B.; Liu, X. Cementitious activity of iron ore tailing and its utilization in cementitious materials, bricks and concrete. *Constr. Build. Mater.* **2021**, *288*, 123022. [CrossRef]
76. Yang, M.; Sun, J.; Dun, C.; Duan, Y.; Meng, Z. Cementitious activity optimization studies of iron tailings powder as a concrete admixture. *Constr. Build. Mater.* **2020**, *265*, 120760. [CrossRef]
77. Benezet, J.C.; Benhassaine, A. Grinding and pozzolanic reactivity of quartz powders. *Powder Technol.* **1999**, *105*, 167–171. [CrossRef]
78. Fernandez, R.; Martirena, F.; Scrivener, K.L. The origin of the pozzolanic activity of calcined clay minerals: A comparison between kaolinite, illite and montmorillonite. *Cem. Concr. Res.* **2011**, *41*, 113–122. [CrossRef]
79. Tan, X.; Wang, W.; Long, S.; Yang, C.; Xu, F. Effects of calcination on mineralogical properties and reactivity of acidic aluminum sulfate residue. *Mater. Lett.* **2020**, *258*, 126810. [CrossRef]
80. Zhao, S.; Fan, J.; Sun, W. Utilization of iron ore tailings as fine aggregate in ultra-high performance concrete. *Constr. Build. Mater.* **2014**, *50*, 540–548. [CrossRef]
81. Dedavid, B.A.; Gomes, C.I.; Machado, G. *Microscopia Eletrônica de Varredura: Aplicações e Preparação de Amostras: Materiais Poliméricos, Metálicos e Semicondutores*; EDIPUCRS: Porto Alegre, Brasil, 2007. (In Portuguese)
82. Bottino, F.; Milan, J.A.M.; Cunha-Santino, M.B.; Bianchini, I. Influence of the residue from an iron mining dam in the growth of two macrophyte species. *Chemosphere* **2017**, *186*, 488–494. [CrossRef]
83. Gomes, M.I.; Gonçalves, T.D.; Faria, P. Unstabilized Rammed Earth: Characterization of Material Collected from Old Constructions in South Portugal and Comparison to Normative Requirements. *Int. J. Archit. Herit.* **2013**, *8*, 185–212. [CrossRef]
84. Avila, F.; Puertas, E.; Gallego, R. Characterization of the mechanical and physical properties of unstabilized rammed earth: A review. *Constr. Build. Mater.* **2021**, *270*, 121435. [CrossRef]
85. Eusébio, A.P.J. Reabilitação e Melhoramento de Paredes de Terra Crua-Taipa. Master's Thesis, Universidade Técnica de Lisboa, Instituto Superior Técnico, Lisboa, Portugal, 2001. (In Portuguese).
86. Jayasinghe, C.; Kamaladasa, N. Compressive strength characteristics of cement stabilized rammed earth walls. *Constr. Build. Mater.* **2007**, *21*, 1971–1976. [CrossRef]
87. Norma, E. *080 Diseño y Construcción con Tierra Reforzada*; Ministerio de Vivienda, Construcción y Saneamiento: Lima, Perú, 2017; Available online: https://www.sencico.gob.pe/descargar.php?idFile=3478 (accessed on 10 August 2022).
88. *NZS 4297*; Engineering Design of Earth Buildings. Earth Building Association of New Zealand: Auckland, Nova Zealand, 1998.